Publication information

Title	Capacity Region of a MAC With a Wireless-Powered DF Relay-to-Destination Link
Author(s)	Zhou, Runfa; Cheng, Roger S.
Source	2017 IEEE 86th Vehicular Technology Conference (VTC2017-Fall), Toronto, Canada, 24-27 September 2017
Version	Pre-published version
DOI	Nil
Publisher	Nil

Copyright information

Notice

Capacity Region of a MAC With a Wireless-Powered DF Relay-to-Destination Link

Runfa Zhou, *Student Member, IEEE* and Roger S. Cheng, *Fellow, IEEE*
Department of Electronic and Computer Engineering
The Hong Kong University of Science and Technology, Hong Kong
{rzhou,eecheng}@ust.hk

***Abstract*—We consider a two-user multiple access channel (MAC) with a wireless-powered relay-to-destination (R-D) link, where the relay adopts the decode-and-forward (DF) relaying strategy and operates in half-duplex mode. Each frame is divided into three phases. In the first phase, the relay harvests energy from a radio frequency (RF) signal sent by a dedicated Power Beacon (PB). The relay then receives information from user nodes in the second phase and forwards it to the destination in the third phase using its harvested energy. We are interested in the system performance with the wireless-powered relay, as compared to the conventional MAC with an R-D link. In particular, we investigate the sum-rate and capacity region of the MAC with wireless-powered relay by jointly optimizing the time scheduling and transmit powers at the user nodes. The optimal scheduling and power allocations are obtained for both the sum-rate and the boundary points on the capacity region. Simulation results validate our theoretical analysis and demonstrate the effectiveness of our proposed solution.**

I. Introduction

Radio frequency (RF) energy harvesting has attracted significant attentions in recent years, for its advantages in transferring energy and information at the same time, and its capability of prolonging battery lifetime of devices [1]. This is especially important for low power consumption networks, such as sensor networks, which play an important role in future technologies in the internet of things (IoT) or machine-to-machine communications [2].

In the literature, there are two paradigms for wireless information and power transfer: Simultaneous wireless information and power transfer (SWIPT) and wireless powered communication networks (WPCN). SWIPT focuses on information transmission and power transfer at the same time [3]. However, limitations in implementation may prevent decoding information and harvesting energy from the same signal simultaneously. Many methods have been proposed to cope with this situation, for instance, multiplexing information receiving and energy harvesting in time, power, spatial, or frequency domains. These different protocols present many interesting problems in system optimization.

Different from SWIPT, which emphasizes the simultaneous transmission of information and energy, WPCN concentrates on the system design of wireless-powered nodes. In such systems, wireless-powered nodes powered entirely on their harvested energy which either comes from the same information source or a dedicated power beacon. The difference between a WPCN and a conventional communication network is the adoption of wireless-powered nodes, which considerably alters the system characteristics. Therefore, it is meaningful to investigate the optimal system design under the new network models. Various network models have been considered in the literature, including point-to-point channels, one-way relay channels and two-way relay channels, where either the relay is wireless powered or the relay acts as a power beacon and the user nodes are wireless powered [4]. Authors in [5]–[7] have considered optimal system designs in MAC with energy harvesting. However, all these works in MAC consider one-hop communication, and the user nodes are wireless powered. Few works have considered a multiple access channel (MAC) with a wireless-powered relay and hence a wireless-powered relay-to-destination (R-D) link. Therefore, it seems interesting to study the performance of such a system.

In this paper, we consider a two-user MAC with a wireless-powered relay harvesting energy from a dedicated power beacon and use the harvested power to forward information to the destination. We investigate the sum-rate maximization problem and find the capacity region under the energy causality and users' power constraints. We obtained the optimal solutions in semi-closed form, and simulation results verify our theoretical analysis.

II. System Model

As shown in Fig. 1, we consider a two-user MAC with a wireless-powered relay, where the relay is denoted as R, the destination D and two user nodes U_1 and U_2, respectively. It is assumed that the relay harvests energy from a dedicated Power Beacon (PB), which has a maximum transmission power P_{pb}. U_1 and U_2 have a steady power supply and their transmission powers, p_1 and p_2, are upper bounded by P_1 and P_2, respectively. All nodes are equipped with a single antenna.

As depicted in Fig. 2, we adopt the harvest-then-transmit protocol [8], and each frame is divided into three phases, starting from the first phase in which the relay harvests energy from the power beacon, to the second phase in which the relay receives information from the users, followed by the last phase in which the relay decodes information and forwards it to the destination. It is assumed that the decode-and-forward relaying strategy is adopted and the relay operates in half-duplex mode.

This research was supported in part by the Hong Kong Research Grant Council under project number 611613.

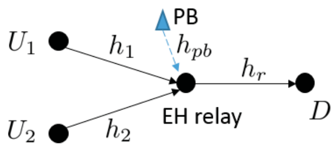

Fig. 1: System model.

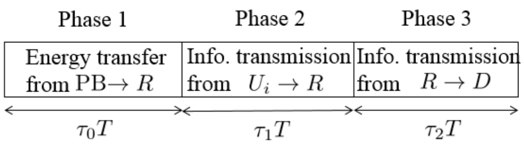

Fig. 2: Frame structure.

Without loss of generality, each frame length is taken as $T = 1$ and the durations of the three phases are denoted as τ_0, τ_1 and τ_2, respectively. Time causality constraint requires that $\tau_0 + \tau_1 + \tau_2 \leq 1$.

We denote by h_1 and h_2 the channel gains from the source nodes to the relay, by h_r the channel gain from the relay to the destination and by h_{pb} the channel gain from the power beacon to the relay. It is assumed that all the channels are quasi-static flat-fading, (i.e., the channel gains remain constant during each block, but change independently from one block to another). For simplicity, we further assume that no direct link exist between the users and the destination and that the relay knows all the channel conditions perfectly at the beginning of each block and makes all the decisions.

In phase 1, the power beacon sends $\sqrt{P_{pb}}x_0$, with $E\left[|x_0|^2\right] = 1$. The received signal at the relay is

$$y_{r1} = \sqrt{P_{pb}h_{pb}}x_0 + n_1. \tag{1}$$

It is assumed that P_{pb} is large and the energy harvested from the noise can be neglected. Therefore, the amount of harvested energy at the relay in phase 1 equals

$$E_h = \eta h_{pb} P_{pb}(1 - \tau_1 - \tau_2), \tag{2}$$

where η represents the energy harvesting efficiency at the relay and it is assumed to be a constant for convenience.

In phase 2, the user nodes send signals $u_i = \sqrt{p_i}x_i$, with $E\left[|x_i|^2\right] = 1$, $i = 1, 2$. The relay receives

$$y_{r2} = \sqrt{h_1 p_1}x_1 + \sqrt{h_2 p_2}x_2 + n_2, \tag{3}$$

where $n_2 \sim \mathcal{CN}(0, \sigma^2)$, a circularly symmetric complex Gaussian (CSCG) random variable with zero mean and variance σ^2. Using Succesive Interference Cancellation (SIC) at the relay and without loss of generality $h_1 > h_2$, the relay decodes user 2's information first and cancels it from the signal before decoding user 1's information. The case that $h_1 \leq h_2$ can be solved similarly. The achievable rates from the users to the relay under this decoding order are given as

$$r_{11} = \tau_1 \log_2\left(1 + \frac{h_1 p_1}{\sigma^2}\right) \tag{4}$$

$$r_{21} = \tau_1 \log_2\left(1 + \frac{h_2 p_2}{\sigma^2 + h_1 p_1}\right). \tag{5}$$

In phase 3, the relay re-encodes and transmits x_r to the destination. At the end of phase 3, the destination decodes the users' information and the end-to-end user rates are expressed as

$$R_1 = \min\{r_{11}, r_{12}\} \tag{6}$$

$$R_2 = \min\{r_{21}, r_{22}\}. \tag{7}$$

with the rate constraint of the relay-to-destination link, which is given by $r_{12} + r_{22} \leq \tau_2 \log_2\left(1 + h_r p_r/\sigma_d^2\right)$ and the relay's power constraint $p_r \leq (1 - \tau_1 - \tau_2)\eta h_p P_{pb}/\tau_2$.

As can be seen from the above, the decoding order does not affect the sum-rate, and thus the end-to-end sum-rate can be expressed as

$$R_{sum} = \min\left\{\tau_1 \log_2\left(1 + \frac{h_1 p_1 + h_2 p_2}{\sigma^2}\right),\right.$$
$$\left.\tau_2 \log_2\left(1 + \frac{h_r p_r}{\sigma_d^2}\right)\right\}. \tag{8}$$

III. Sum-Rate Maximization and The Capacity Region

In this section, we investigate the sum-rate maximization problem and the capacity region by jointly considering time scheduling and power allocations. We first look into the sum-rate maximization problem, which gives some insight for characterizing the capacity region.

For notation symplicity, we define $\mathbb{S}_\tau = \{(\tau_1, \tau_2) : \tau_1 + \tau_2 < 1, \tau_1, \tau_2 > 0\}$, $\mathbb{S}_{\mathbf{p}} = \{\mathbf{p} : p_1 \leq P_1, p_2 \leq P_2,\ p_1, p_2, p_r \geq 0\}$, $\mathbb{S}_{\mathbf{p}_s} = \{(p_1, p_2) : p_1 \leq P_1, p_2 \leq P_2,\ p_1, p_2 \geq 0\}$, where $\mathbf{p} = [p_1, p_2, p_r],\ \mathbf{p}_s = [p_1, p_2]$.

A. Sum-Rate Maximization

The problem is formulated as follows:

$$(P1): \quad \max_{\tau \in \mathbb{S}_\tau, \mathbf{p} \in \mathbb{S}_{\mathbf{p}}} \quad R_{sum} \tag{9}$$

$$\text{s.t.} \quad p_r \leq (1 - \tau_1 - \tau_2)\eta h_p P_{pb}/\tau_2 \tag{10}$$

First we have the following lemma.

Lemma 3.1: The optimal values of the power at the source nodes and the relay all achieve the maximum; i.e.,

$$p_1^* = P_1,\ p_2^* = P_2, \tag{11}$$

$$p_r^* = \frac{(1 - \tau_1 - \tau_2)}{\tau_2}\eta h_p P_{pb}. \tag{12}$$

Proof: This can be proved by contradiction. If for the optimal solution, p_1 or p_2 is less than its maximum, then we can always increase the power and decrease τ_1, which will result in a larger R_{sum}. Similarly, if p_r is less than its maximum, we can increase τ_1 and get a larger R_{sum}, which is a contradiction. ■

Based on the above lemma and the variable substitution $E_r = p_r\tau_2$, we reformulate the problem into a convex one by using the epigraph form:

$$
\begin{aligned}
(P2): \quad & \max_{\tau\in\mathbb{S}_\tau, E_r} \quad r && (13)\\
\text{s.t.} \quad & r \le c_1\tau_1 && (14)\\
& r \le \tau_2\log_2\left(1+\frac{h_r E_r}{\sigma_d^2\tau_2}\right) && (15)\\
& E_r \le (1-\tau_1-\tau_2)\eta h_p P_{pb} && (16)\\
& E_r \ge 0 && (17)
\end{aligned}
$$

$(P2)$ is convex since the objective function is linear and all the constraints and the feasible set are convex. We only need to check the convexity of constraint (15) by taking its Hessian, and the rest are all linear constraints. Next we solve the problem by its K.K.T. conditions [9], and the results are concluded in the following theorem.

Theorem 3.1: The maximum sum rate always makes $c_1\tau_1^* = \tau_2^*\log_2\left(1+\frac{h_r E_r}{\sigma_d^2\tau_2^*}\right)$, and the optimal τ_1^* and τ_2^* are given as follows:

$$\tau_1^* = \frac{\eta h_p P_{pb}}{\eta h_p P_{pb} + \frac{c_1(m+\eta h_p P_{pb})}{\log_2(1+c_2 m)}} \quad (18)$$

$$\tau_2^* = \frac{c_1}{\log_2(1+c_2 m)}\tau_1^*, \quad (19)$$

where $c_1 = \log_2\left(1+\frac{h_1P_1+h_2P_2}{\sigma^2}\right), c_2 = h_r/\sigma_d^2$ and m is the unique solution of the equation $\log(1+c_2x) - \frac{c_2}{1+c_2x}(x+\eta h_p P_{pb}) = 0$.

Proof: The Lagrangian is

$$
\begin{aligned}
\mathcal{L} \;=\; & r - \lambda_1(r-\tau_1c_1) - \lambda_2(r-\tau_2\log_2(1+c_2E_r/\tau_2)\\
& -\lambda_3[E_r-(1-\tau_1-\tau_2)h_pP_{pb}]) - \lambda_4(\tau_1+\tau_2-1).
\end{aligned}
$$

Taking the derivatives of $\mathcal{L}$ with respect to r, τ_1, τ_2 and E_r and setting them all to zero, together with the complementary slackness conditions and the fact that τ_1, τ_2, p_1 and p_2 are all non-negative, we can reach equations (18) and (19). ∎

We are interested in how the values of P_1, P_2 and P_{pb} affect the optimal values of τ_1, τ_2 and the sum-rate.

Corollary 3.2: When P_1 or P_2 increases, τ_1 decreases and τ_0, τ_2 increase. And $\lim_{c_1\to 0}\tau_1^* = 1$, $\lim_{c_1\to 0}\tau_2^* = 0$.

Proof: This can be directly seen from Theorem 3.1. ∎

Corollary 3.3: $\lim_{P_{pb}\to\infty}\tau_1^* = 1$ and $\lim_{P_{pb}\to\infty}\tau_2^* = 0$.

Proof: The key is to show that $\lim_{P_{pb}\to\infty} m/P_{pb} = 0$. When $P_{pb} \to \infty$, we also have $m \to \infty$. Then $\lim_{P_{pb}\to\infty} m/P_{pb} = \lim_{m\to\infty}\frac{mc_2\eta h_p}{(1+c_2m)\log(1+c_2m)-c_2m} = \lim_{m\to\infty}\frac{c_2\eta h_p}{\frac{1}{m}\log(1+c_2m)+c_2\log(1+c_2m)-c_2} = 0$. Therefore, we have $\lim_{P_{pb}\to\infty}\tau_1^* = \lim_{m\to\infty}\frac{\eta h_p}{\eta h_p + \frac{c_1(m/P_{pb}+\eta h_p)}{\log_2(1+c_2m)}} = 1$, $\lim_{P_{pb}\to\infty}\tau_2^* = \lim_{P_{pb}\to\infty}\frac{c_1\eta h_p P_{pb}}{\eta h_p P_{pb}\log_2(1+c_2m)+c_1(m+\eta h_p P_{pb})} = \lim_{m\to\infty}\frac{c_1\eta h_p}{\eta h_p\log_2(1+c_2m)+c_1(m/P_{pb}+\eta h_p)} = 0$. ∎

For the maximal sum-rate, as $R_{sum}^* = \tau_1^* c_1$, when the source nodes' maximum transmission power increases, the optimal sum-rate also increases despite the fact that τ_1^* decreases. When P_{pb} increases, the optimal sum-rate also increases.

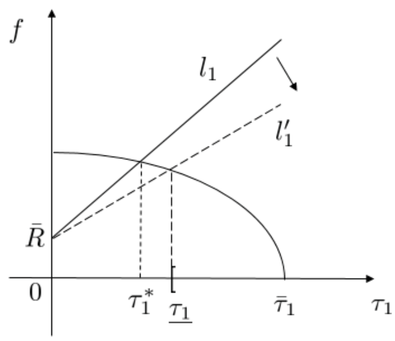

Fig. 3: The relationship between r_{11} and R_{rd} with respect to τ_1.

B. Capacity Region

Here we assume $h_1 \ge h_2$, and thus user 2's information is firstly decoded at the relay if not otherwise specified. The case that user 1's information is decoded first is similar, and thus it is omitted due to space limitation. The problem can be formulated as follows:

$$
\begin{aligned}
(P3): \quad & \max_{\tau\in\mathbb{S}_\tau, \mathbf{p}\in\mathbb{S}_\mathbf{p}} \quad R_1 && (20)\\
\text{s.t.} \quad & R_1 \le \tau_1\log_2\left(1+\frac{h_1p_1}{\sigma^2}\right) && (21)\\
& \bar{R} \le \tau_1\log_2\left(1+\frac{h_2p_2}{\sigma^2+h_1p_1}\right) && (22)\\
& r_{12}+r_{22} \le \tau_2\log_2\left(1+\frac{h_rp_r}{\sigma_d^2}\right) && (23)\\
& p_r \le \frac{(1-\tau_1-\tau_2)}{\tau_2}\eta h_p P_{pb} && (24)
\end{aligned}
$$

where $R_1 = \min\{r_{11}, r_{12}\}$ and $R_2 = \min\{r_{21}, r_{22}\}$.

First, we have the following lemma.

Lemma 3.2: The optimal solution satisfies $p_r^* = \frac{(1-\tau_1-\tau_2)}{\tau_2}\eta h_p P_{pb}$, $r_{12}^* = R_1$ and $r_{22}^* = \bar{R}$.

Proof: This again can be proved by contradiction, and the details are omitted due to space limitation. ∎

Based on Lemma 3.2, the problem can be rewritten as follows.

$$
\begin{aligned}
(P4): \quad & \max_{\tau\in\mathbb{S}_\tau, \mathbf{p}_s\in\mathbb{S}_{\mathbf{p}_s}} \quad R_1 && (25)\\
\text{s.t.} \quad & R_1 \le \tau_1\log_2\left(1+\frac{h_1p_1}{\sigma^2}\right) && (26)\\
& \bar{R} \le \tau_1\log_2\left(1+\frac{h_2p_2}{\sigma^2+h_1p_1}\right) && (27)\\
& R_1 + \bar{R} \le R_{rd} && (28)
\end{aligned}
$$

where $c_3 = \eta h_r h_p P_{pb}/\sigma_d^2$ and $R_{rd} = \tau_2\log_2\left(\frac{c_3(1-\tau_1-\tau_2)}{\tau_2}\right)$.

Note that for a given feasible $\bar{R}$, the constraints for R_1 are irrelavent to p_2. As depicted in Fig. 3, the key observation is that due to the monotonicities of r_{11} and R_{rd} with respect to τ_1, there must exist a unique τ_1^* such that $r_{11} = R_{rd}$ and that achieves the maximum R_1. Moreover, the slope of l_1, which is determined by $\log_2\left(1+h_1p_1/\sigma^2\right)$, affects the optimal R_1. Specifically, l_1 with a larger slope results in a larger R_1, as the intersection of these two curves will move to the left. Therefore, p_1 should be P_1 if possible. However, the infeasibility may be caused by constraint (27), which requires $\tau_1 \geq \underline{\tau_1}$ and $\underline{\tau_1} = \bar{R}/\log_2(1+\frac{h_2 p_2}{\sigma^2+h_1 p_1})$, since τ_1^* may be less than $\underline{\tau_1}$. If $\tau_1^* < \underline{\tau_1}$, to ensure feasibility, p_1 has to be decreased until $\tau_1^* = \underline{\tau_1}$. Since, as shown in Fig. 3, with p_1 decreasing, l_1 moves to l_1', τ_1^* increases and $\underline{\tau_1}$ decreases.

Naturally, we start the analysis from the relationship between τ_1^* and $\underline{\tau_1}$. We conclude the results in the following theorem.

Theorem 3.4: For the points on part AB of the capacity region, as shown in Fig. 7, the rate pair is $(k_1\tau_1^*,\ \bar{R})$. The optimal power allocation at the source nodes satisfies

$$\begin{cases} p_1^* = P_1, \\ p_2^* = (2^{\bar{R}/\tau_1^*}-1)(\sigma^2+h_1P_1)/h_2, \end{cases} \tag{29}$$

and the optimal scheduling is given by

$$\tau_1^* = \tau_1^a,\ \ \tau_2^* = \tau_2^a, \tag{30}$$

where τ_1^a corresponds to the maximal value of $g_1(x) = 1+(1-k_2)x/k_2 - x\cdot W_0\left(\frac{k_1\ln 2}{k_2}2^{-k_1+\frac{k_1}{k_2}+\frac{k_1+\bar{R}}{x}}\right)/(k_1\ln 2)$, $W_0(x)$ is the principal branch of the Lambert W-function [10] ,and τ_2^a corresponds to x^*, which gives the maximum value of $g_1(x)$. $k_1 = \log_2\left(1+h_1P_1/\sigma^2\right)$ and $k_2 = \eta h_r h_p P_{pb}/\sigma_d^2$.

Proof: When $\bar{R}$ is small, $\underline{\tau_1}$ is small and $p_1 = P_1$ can be satisfied without violating $\tau_1^* \geq \underline{\tau_1}$. According to Fig. 3, the optimal τ_1 should be the intersection of the two curves, which makes $\tau_1 = 1+(1-k_2)\tau_2/k_2 - \tau_2\cdot W_0\left(\frac{k_1\ln 2}{k_2}2^{-k_1+\frac{k_1}{k_2}+\frac{k_1+\bar{R}}{\tau_2}}\right)/(k_1\ln 2)$. And $p_2^* = (2^{\bar{R}/\tau_1^*}-1)(\sigma^2+h_1P_1)/h_2$, which is given by constraint (27). τ_1^* can be found using the bisection method. However, when $\bar{R}$ keeps increasing, on the one hand, the intersection in Fig. 3 moves to the left, and on the other hand, the lower bound of the feasible τ_1 moves to the right. Therefore, there exists a critical value of $\bar{R}^c$, at which point constraint (27) is met with equality and $p_1 = P_1, p_2 = P_2$. For $\bar{R} > \bar{R}^c$, p_1 has to be decreased to make l_1 move to l_1' and $\underline{\tau_1}$ move to the left to guarantee the feasibility of the problem. Moreover, we point out that for $\bar{R} = \bar{R}^c$, the rate pair is the same as the result of the sum-rate maxmization problem, which corresponds to point B in Fig. 7. This is not diffcult to understand since we have proved in the previous sub-section that there exists a unique solution for the optimal sum-rate and the rate pair at point B is also optimal under the same system settings. Thus these two have to be the same. Therefore, this theorem gives the capacity region for $\bar{R} \leq \bar{R}^c$, which corresponds to part AB in Fig. 7. ■

Subsequently, we claim that for $\bar{R} > \bar{R}^c$, the rate pairs produced under the decoding order that user 2's information is decoded first lie strictly inside the capacity region. This is because, for $\bar{R} > \bar{R}^c$, $p_1 < P_1$ and the corresponding sum-rate has to be less than the optimal. Therefore, for deriving the capacity region, the case that $\bar{R} > \bar{R}^c$ under the assumption that user 2's information is decoded first does not need to be considered. In fact, segment BC is achieved by time sharing between the two decoding orders. And part CD corresponds to the case when user 1's information is decoded first. At this point, we have derived the whole capacity region.

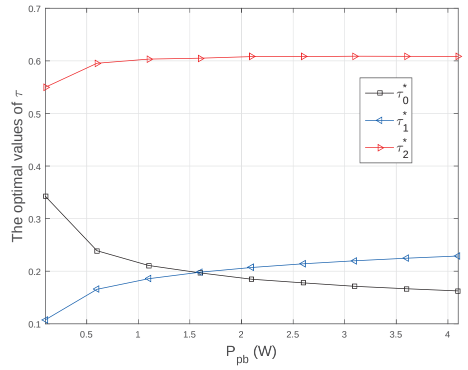

Fig. 4: The optimal values of $\boldsymbol{\tau}$ versus PB's maximum power P_{pb} with $P_s = 1W$.

Remark The two corner points (B and C) correspond to rate pairs $\left(\tau_1^*\log_2(1+h_1P_1/\sigma^2), \tau_1^*\log_2(1+\frac{h_2P_2}{\sigma^2+h_1P_1})\right)$ and $\left(\tau_1^*\log_2(1+\frac{h_1P_1}{\sigma^2+h_2P_2}), \tau_1^*\log_2(1+h_2P_2/\sigma^2)\right)$, respectively. And with $\tau_1^* \to 1$, the capacity region converges to the case of the conventional relay. That is to say, a larger P_{pb} or h_p helps to enlarge the capacity region. A small c_1, which means a low signal-to-noise ratio (SNR) at the source to relay link would also help to decrease the gap between those two capacity regions.

IV. Simulation Results

In this section, we validate our analysis through simulations. We let the bandwidth be 1 MHz, and the channel power gains $h_i = 10^{-3}\lambda d_i^{-\theta},\ i = 1,2,r,p$, where λ is an exponentially distributed random variable with mean 1, d_i is the distance between network nodes, and θ is the path-loss exponent. We let $\sigma^2 = \sigma_d^2 = -110$ dBm for simplicity. In the rest, we denote $\boldsymbol{\tau} = [\tau_0, \tau_1, \tau_2]$. The results are generated by averaging over 100 realizations.

First we investigate the optimal scheduling for sum-rate maximization. In this simulation, we set $d_1 = d_2 = d_r = 10m$, $d_p = 2m$ and $\theta = 2$. Fig. 4 gives the optimal values of τ_0, τ_1 and τ_2 versus P_{pb}. It is shown that with the increase of P_{pb}, τ_1^* and τ_2^* increase, and this is because a larger transmit power can shorten the power transmission phase.

Fig. 5 shows the optimal values of τ_0, τ_1 and τ_2 versus the user nodes' maximum transmission power. Here we assume $P_1 = P_2 = P_s$ for simplicity. As analysed in Corollary 3.2, when P_s increases, c_1 increases, τ_1^* decreases, and τ_0^* and τ_2^* increase. However, as shown in the figure, the optimal scheduling is not affected too much by P_s. This happens when $\frac{c_1^2(1+c_2m)}{\eta h_p P_{pb} c_2} \gg 1$, which means the SNR of the R-D link is much smaller than that of the source-to-relay link.

Fig. 6 depicts the relationship between the optimal sum-rate and P_s, P_{pb} and the sum-rate under different schemes. We compare the results of our proposed scheme with those of

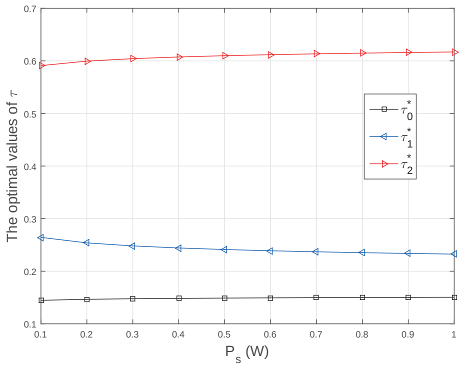

Fig. 5: The optimal values of $\boldsymbol{\tau}$ versus the source nodes' maximum power P_s with $P_{pb} = 4W$.

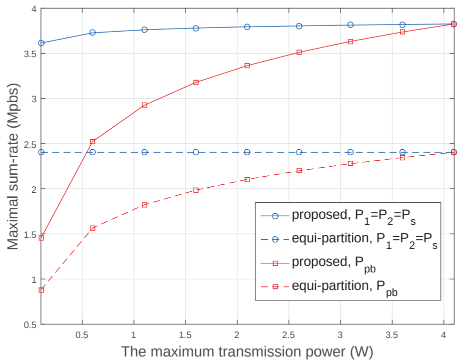

Fig. 6: The maximal sum-rate versus the source nodes' maximum power P_s and P_{pb}.

the benchmark scheme $\tau_0 = \tau_1 = \tau_2 = 1/3$. It is interesting to see that P_{pb} influences the sum-rate in a much more severe way than P_s. This is also quite intuitive, as the bottleneck of the proposed system is the amount of energy that the wireless powered relay can harvest. It is observed from the figure that our proposed scheme has a significant improvement in sum-rate compared to the benchmark scheme.

Finally, in Fig. 7, we provide the entire capacity regions under different P_{pb}. Here we let $h_1 = 0.5, h_2 = 0.2, h_r = 1$ and $P_s = 1W$ for illustration. The outer polygon is the capacity region for the conventional relay case where the relay's maximum power is assumed to be infinitely large. It can be seen that the capacity region enlarges with P_{pb} and the tendency of parts AB and CD also changes. With P_{pb} getting larger, AB becomes flatter and CD becomes deeper. The capacity region of the system with the wireless powered relay finally converges to that in the case with a conventional relay. This is not hard to understand as for a very large P_{pb}, the relay can harvest a sufficient amount of energy in negligible time and the difference between these two systems vanishes. Moreover, AB and CD seem linear in the simulation, but due to the high complexity of $g_1(x)$, deriving it analytically is quite challenging. Therefore we leave it for future consideration.

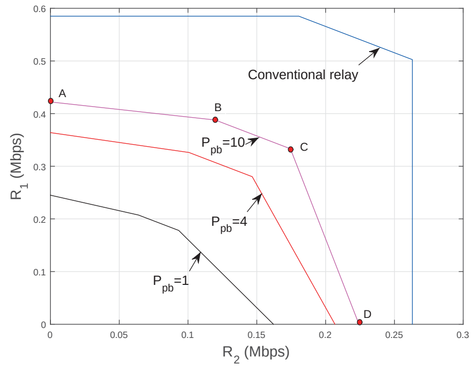

Fig. 7: The capacity regions versus P_{pb} with $h_1 = 0.5, h_2 = 0.2, h_r = 1, P_s = 1W$.

V. Conclusion

In this paper, we have investigated the sum-rate maximization and the capacity region of a two-user MAC with a wireless powered relay, by jointly optimizing the time scheduling and the transmit powers at user side. We have recast the sum-rate maximization into a convex problem and obtained the semi-closed form optimal solution, while for the capacity region, we have simplified the problem by looking into its structures and finally solved it by the bisection method. Simulation results demonstrate the correctness of our theoretical analysis and the effectiveness of our proposed solutions.

References

[1] S. Inoue, Y. Kakuda, K. Kurokawa, and T. Dohi, "A method to prolong the lifetime of sensor networks by adding new sensor nodes to energy-consumed areas," in *Proc. 2nd Int. Symp. Aware Computing (ISAC)*, pp. 332–337, Nov. 2010.

[2] X. Lu, P. Wang, D. Niyato, D. I. Kim and Z. Han, "Wireless networks with RF energy harvesting: A contemporary survey," *IEEE Commun. Surveys Tuts.*, vol. 17, no. 2, pp. 757–789, Second quarter 2015.

[3] R. Zhang and C. K. Ho, "MIMO broadcasting for simultaneous wireless information and power transfer," *IEEE Trans. Wireless Commun.*, vol. 12, no. 5, pp. 1989–2001, May 2013.

[4] R. Zhou and R. S. Cheng, "Optimal scheduling and power allocation for wireless powered two-way relaying systems," in *Proc. IEEE WCNC,* Doha, Qatar, pp. 1–6, Apr. 2016.

[5] R. A. Raghuvir, D. Rajan and M. D. Srinath, "Capacity of the Multiple Access Channel in energy harvesting wireless networks," in *Proc. IEEE WCNC,* Paris, France, pp. 898–902, Apr. 2012.

[6] K. Tutuncuoglu and A. Yener, "Multiple access and two-way channels with energy harvesting and bi-directional energy cooperation," in *Information Theory and Applications Workshop (ITA),* pp. 1–8, Feb. 2013.

[7] Z. Hadzi-Velkov, N. Zlatanov and R. Schober, "Multiple-access fading channel with wireless power transfer and energy harvesting," in *IEEE Commun. Lett.,* vol. 18, no. 10, pp. 1863–1866, Oct. 2014.

[8] H. Ju and R. Zhang, "Throughput maximization in wireless powered communication networks," in *Proc. IEEE GLOBECOM*, pp. 4086–4091, Dec. 2013.

[9] S. Boyd, and L. Vandenberghe, *Convex Optimization*, Cambridge University Press, 2004.

[10] E. W. Weisstein, "Lambert W-function, *MathWorld – A Wolfram Web Resource,* http://mathworld.wolfram.com/LambertWFunction.html.